Vortex dynamics for low-κ type-II superconductors

X. B. Xu,[1,*] H. Fangohr,[2] Z. H. Wang,[1] M. Gu,[1] S. L. Liu,[3] D. Q. Shi,[4] and S. X. Dou[4]

[1]*National Laboratory of Solid State Microstructures, Department of physics, Nanjing University, Nanjing 210093, People's Republic of China*
[2]*School of Engineering Sciences, University of Southampton, Southampton SO17 1BJ, United Kingdom*
[3]*College of Science, Nanjing University of Posts and Telecommunications, People's Republic of China*
[4]*Institute for Superconducting and Electronic Materials, University of Wollongong, New South Wales 2522, Australia*

Based on a model appropriate for "marginally type-II" superconducting system, we study the dynamics of vortices with competing interactions by Langevin dynamics simulation. In addition to pinned states and plastic flow, we find that the moving vortex system forms ordered bubble configurations and stripe structures, depending on pinning strength and driving force. The vortex system exhibits a marked hysteresis in its velocity-force characteristic, which results from a dynamical stripe reordering due to intervortex attraction.

I. INTRODUCTION

A rich variety of physical and chemical systems display self-organization and structural modulation, originating from a compromise of the competing long-range repulsive and short-range attractive interactions.[1] Although the mechanisms of the interactions may be different from system to system, these systems exhibit some common structural characteristics, including stripes and circular droplets (bubbles) in two-dimensional systems and sheets, tubes, and spherical droplets embedded in a homogeneous three-dimensional matrix, see, for example, Ref. 1 and references therein. The period of the modulated structures can be tuned by changing the relative strengths of the competing interactions or by controlling external parameters such as temperature or applied magnetic or electric fields.[2–6]

Such modulated structures can also be found in superconducting systems: the intermediate state in type-I superconductors,[7] and the intermediate-mixed state in low-κ type-II superconductors.[7–10] For a type-I superconductor, both droplet and stripe patterns are observed in a slab geometry due to the competition between the interface energy and a demagnetizing field. For a low-κ type-II superconductor, such as Nb, V, Tc, and Pb alloys,[7] the two-band superconductor MgB$_2$,[11] and the spin-triplet superconductor Sr$_2$RuO$_4$,[12] the superconducting vortices form islands or lamellas of regions in the Meissner state submerged in the normal regions filled with vortices, or such normal regions surrounded by Meissner state regions. Particularly, two kinds of vortex superlattices can be found for the low-κ superconductors, (i) the parallel stripe-like Shubnikov domains embedded in the Meissner phase for Nb single crystals,[13] (ii) the ordered bubble-like Shubnikov domains embedded in a Meissner phase for high-purity Nb foil, as shown in Fig. 4 in Ref. 10. The intermediate-mixed state has been explained by the appearance of a long-range vortex attraction that causes an S-shape (unstable) magnetization curve from which the equilibrium states are obtained by a Maxwell construction.[11,14–18] The observations of bubble-like or stripe-like or other irregular vortex domains indeed show the existence of the intervortex attraction for low-κ type-II superconductors, but the presence of long-range order between vortex domains means that the long-range interaction between vortices should be repulsive rather than attractive. Therefore, to study the statics and the dynamics in the vortex systems

with κ close to $1/\sqrt{2}$, one has to consider the long-range repulsion in addition to the attraction between vortices. In our previous work,[19] a phenomenological model was proposed to study the static phase behaviors of the vortex system, in which the vortices interact with each other through a short-ranged attraction and a long-ranged repulsion. This model system can reproduce all of the well-known vortex phases such as the Abrikosov mixed phase and the intermediate-mixed phase, depending on temperature, magnetic field, and κ. However, the dynamics of the vortices with competing interactions in a superconducting system with quenched disorders has not been investigated to the best of our knowledge. It is not clear how the disorders affect the formation of moving states for such vortex systems, and what types of dynamic phases exist as a function of driving force.

In this work, we study the nonequilibrium driven phases for the vortices with competing interactions at zero temperature based on our model system with Langevin dynamics simulation. Depending on pinning strength and driving force, we find that the vortex system displays a variety of dynamic phases: pinned state and plastic flow for lower driving forces, and ordered moving bubbles and ordered moving stripes for larger driving forces. While the driving force can induce order at the macro scale (which is realized through the appearance of bubbles or stripes), the vortices inside each bubble and stripe remain disordered. We have found no evidence that the local order within each bubble or stripe could be introduced by varying the strength of the driving force. In addition, we find that the vortex system shows a marked hysteresis in its velocity-force characteristic. This is associated with the reordering of the system from a disordered configuration (which results in slower motion) into a stripe domains (which results in faster motion) for identical driving forces. The reordering takes place at large driving forces.

II. SIMULATION

The overdamped Langevin equation of motion for a vortex at position $\mathbf{r}_i$ is[20]

$$\mathbf{F}_i = \sum_{j}^{N_v} \mathbf{F}^{vv}(\mathbf{r}_i - \mathbf{r}_j) + \sum_{k}^{N_p} \mathbf{F}^{vp}(\mathbf{r}_i - \mathbf{r}_k^p) + \mathbf{F}^L = \eta \frac{d\mathbf{r}_i}{dt},$$

where $\mathbf{F}_i$ is the total force acting on vortex i, $\mathbf{F}^{vv}$ and $\mathbf{F}^{vp}$ are the forces due to vortex-vortex and vortex-pin interactions, respectively, $\mathbf{F}^L$ is the driving force, η is the Bardeen-Stephen friction coefficient, N_v is the number of vortices, N_p is the number of pinning centers, and $\mathbf{r}_k^p$ is the position of the kth pinning center. The effective interaction between two vortices is[19]

$$F^{vv}(\mathbf{r}) = \frac{\phi_0^2 s}{2\pi\mu_0\lambda^3}\left[\frac{\lambda}{r} - q\exp\left(-\frac{r}{\xi}\right)\right],$$

where ϕ_0 is the flux quantum, s is the length of the vortex, μ_0 is the vacuum permeability, λ is the London penetration depth, and ξ is the effective coherence length, The first term is a long-range repulsion via the logarithmic form potential, which is commonly used to calculate the vortex-vortex interaction in high-κ type-II superconductors,[21] and the second term is the short-ranged vortex attraction of an exponential form. The parameter q reflects the relative strength of the attraction to repulsion interactions. We employ periodic boundary conditions and cut off the vortex-vortex interaction potential smoothly.[22,23] A pinning center at position r_k^p exerts an attractive force on the vortex at position r_i: $\mathbf{F}^{vp}(\mathbf{r}_i - \mathbf{r}_k^p) = -f_{pv}(r_{ik}/r_p)\exp(-(r_{ik}/r_p)^2)\hat{\mathbf{r}}_{ik}$, where f_{pv} tunes the strength of this force and r_p determines its range. $f_{pv} \propto B_{c2}^2(1 - B/B_{c2})\xi^2/\kappa^2$ as core pinning is considered,[24] where $\kappa = \lambda/\xi$. The driving force is applied in x-direction. The average x-component of the velocities of the vortices is $\langle V_x\rangle = \frac{1}{N_v}\sum_i^{N_v} v_{xi}$ which is proportional to the resulting voltage. We normalize lengths by λ_0, forces by $f_0 = (\phi_0^2 s)(2\pi\mu_0\lambda^3)^{-1}$ and time by $\tau_0 = \lambda\eta/f_0$. All quantities shown in the following figures are expressed in these simulation units. The equation of motion is integrated by an Euler scheme with a normalized time step of $\Delta t = 0.005$.[23] The total number of vortices $N_v = 900$ is used in the calculations presented here. For larger systems, similar results are observed. We employ $q = 2.3$, $r_p = 0.2\lambda$, $\xi = 200$ Å, $\lambda = 200$ Å, $s = 12$ Å, and $\eta = 1.4 \times 10^{-17}$ kg/s. In all cases, the vortices are randomly distributed for the initial state of the superconducting system. We calculated the vortex phases by replacing the logarithmic form vortex-vortex potential with the modified Bessel function of the second kind $[K_0(r/\lambda)]$, and found that the simulating results for the modified Bessel function are in qualitatively agreement with those for the logarithmic function. The simulation results in this work are applicable to two-dimensional (thin films, stack of superconducting layers) and quasi-two-dimensional systems (rigid vortex lines).

III. RESULTS AND DISCUSSION

We start by studying the statics of the vortex state with quenched disorder and competing interactions as introduced above. For the sake of simplicity, we demonstrate only the dependence of the equilibrium ordered bubble and stripe states on the density of pinning centers, $n_p = N_p/N_v$, as shown in Fig. 1. For small n_p, it can be seen that the vortex system shows an ordered bubble state (as it would without pinning), except that a few vortices are trapped by the pinning centers, as shown in Fig. 1(a). With increasing n_p, more vortices are pinned, resulting in fuzzier boundaries of the bubbles due to the attractive interactions of pinning centers nearby, as shown
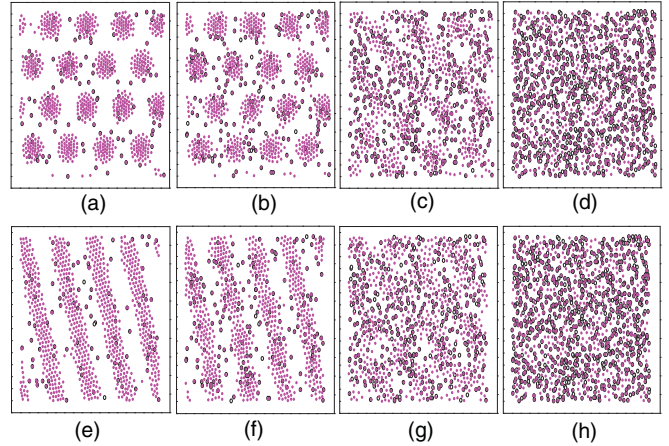

FIG. 1. (Color online) Effect of density of pinning centers (black open circles) n_p on the vortex (magenta solid circles) phase at $f_{pv} = 5f_0$ without an external driving force. The top row shows simulation results for $B = 0.5B_{c2}$ with increasing ratio n_p of number pinning centers to number of vortices: (a) $n_p = 0.1$, (b) $n_p = 0.2$, (c) $n_p = 0.5$, and (d) $n_p = 1$. The vortices for $n_p = 0$ form an ordered bubble state. The bottom row shows simulation results for $B = 0.65B_{c20}$: (e) $n_p = 0.1$, (f) $n_p = 0.2$, (g) $n_p = 0.5$, and (h) $n_p = 1$. The vortices for $n_p = 0$ form an ordered stripe state.

in Fig. 1(b). As n_p is increased further, the pinning centers attract vortices away from the bubbles and the gaps between the bubbles as visible in Figs. 1(a) and 1(b) are increasingly populated with vortices as shown in Fig. 1(c). The additional pinning centers destroy the subtle balance of vortex-vortex repulsion and vortex-vortex attraction which is required to establish the bubble phase, and the vortex system forms interconnected stripe-like domains, as shown in Fig. 1(c). The simulation results show that the pinning destroys the ordered bubble phase and this may explain why the disordered domains of vortices have been frequently observed for low-κ type-II superconductors,[7] while the hexagonally ordered bubble or ordered stripe states were seldom probed in experiments. For still larger n_p, the role of pinning is dominant and thus the vortex system forms a disordered and pinned vortex state, as shown in Fig. 1(d). Similarly, Figs. 1(e)–1(h) show how the ordered stripe state changes successively into the disordered domains and then the disordered single-vortex pinning state with increasing n_p.

We next study the dynamic vortex phases of a low-κ system with quenched disorders. Figure 2 shows the evolution of the vortex state with driving forces at $B = 0.65B_{c2}$ and $f_{pv} = 28.2f_0$. At driving forces below the depinning transition, the vortices are individually trapped by the pinning centers, showing a pinned vortex glass state as seen in Fig. 2(a). With increasing driving force magnitude, a plastic flow state appears: a part of the vortices move in preferred channels, the others remain pinned, as shown in Fig. 2(b). These two vortex states have been well observed in high-κ systems with pure intervortex repulsion.[23,25–31] We thus conclude that for strong pinning and moderate driving forces both for low-κ and high-κ vortex system, the driven vortex states are dominated by pinning and that the details of the intervortex interactions are not so important. Upon further increase of the driving
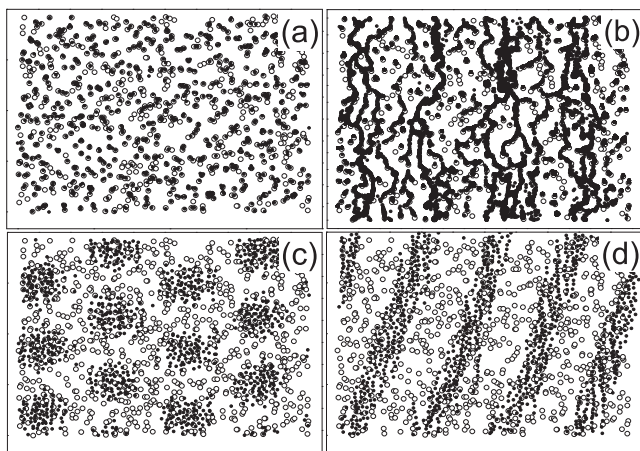
FIG. 2. Vortex configurations for different driving forces at $B = 0.65 B_{c2}$ and $f_{pv} = 28.2 f_0$: (a) $F^L = 0$, (b) $F^L = 20 f_0$, (c) $F^L = 40 f_0$, and (d) $F^L = 100 f_0$. Solid circles and open circles are, respectively, the vortices and the pinning centers.

FIG. 3. Dynamic phase diagram for different pinning strengths and driving forces at $B = 0.65 B_{c2}$. The typical structures of these phases are shown in Figs. 2(a)–2(d).

force, shown in Figs. 2(c) and 2(d), all of the vortices are depinned, and form two kinds of ordered vortex structures: (i) an ordered bubble-like state for comparatively low driving forces [see Fig. 2(c)]; (ii) an ordered stripe-like state for comparatively high driving forces [see Fig. 2(d)]. We have previously shown[19] that, a bubble phase will be observed if the vortex-vortex attraction is large enough (relative to the vortex-vortex repulsion), whereas a stripe phase can be observed for a smaller vortex-vortex attraction [see Fig. 4(b) in Ref. 19]. Thus, the occurrence of the ordered bubble state indicates that the short-range attraction in the vortex-vortex interaction is enhanced due to pinning. Because the effect of pinning is weak for increasing driving force, the effective short-range attraction becomes smaller at larger vortex speed. Thus, the moving ordered bubble state will transit into a moving ordered stripe state at larger vortex speed. In addition, one can note that the vortices inside the moving bubbles or stripes are disordered, indicating that the order of the moving vortices in a short range is determined by pinning and order within each bubble (or stripe) cannot be introduced by a driving force.

Now we construct the phase diagram in the driving force-pinning strength plane at $B = 0.65 B_{c2}$, as shown in Fig. 3. For weak pinning ($f_{pv} \leqslant 3.2 f_0$), the vortex-vortex interactions dominate over the disorders, so the vortex system shows a direct phase transition from pinned ordered bubble phase to moving ordered stripe phase without undergoing intermediate plastic motion. The precise transition driving force is more difficult to identify because of its small magnitude (inline with Refs. 23 and 26). For stronger pinning ($3.2 f_0 < f_{pv} \leqslant 16.0 f_0$), at lower driving forces, the vortex system display a pinned vortex glass and plastic flow with increasing driving force [see Figs. 2(a) and 2(b), respectively]. For higher driving forces, the vortex system forms an moving ordered stripe state due to the dominating intervortex interaction. Upon further increase of pinning strength ($f_{pv} > 16.0 f_0$), between plastic flow and ordered stripe regimes, there exists a hexagonally ordered bubble-like state because of the enhanced vortex-vortex attraction due to pinning.
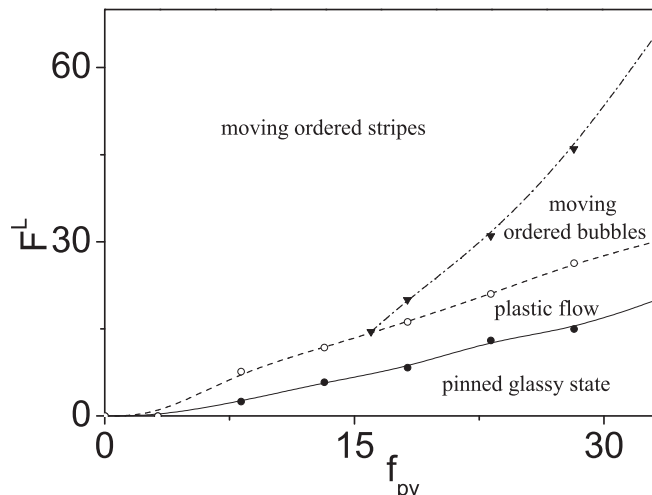
Finally, we study the hysteretic behavior of vortex matter with competing interactions. Fig. 4(a) shows a representative anticlockwise velocity-force curve in one upward/downward force scanning circle for $B = 0.2 B_{c2}$. In order to understand the mechanism responsible for this hysteretic behavior, we examine the vortex configurations in both upward and downward branches at a fixed force at $F^L = 8 f_0$ as shown in Figs. 4(b) and 4(c). We find that the vortices are disordered due to pinning in the upward branch, while become ordered stripe structure in the downward branch. In fact, more pinning centers are ineffective for the vortex stripe configuration in a superconducting system with random pinning centers, leading to a bigger vortex velocity in the downward branch or a velocity-force curve with anticlockwise character. Then we
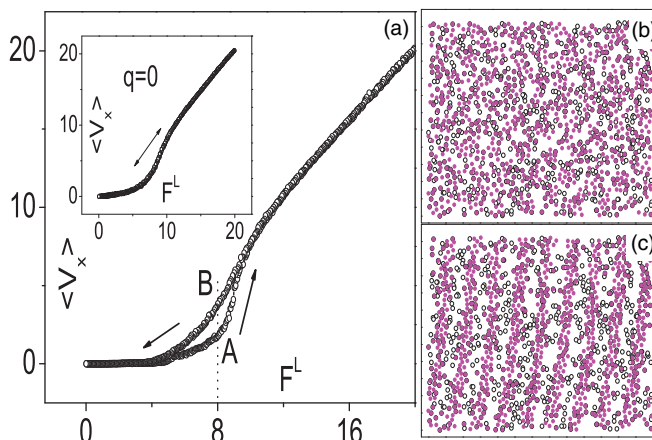

FIG. 4. (Color online) (a) Velocity-force curve for a fixed force scanning rate $dF^L/dt = \pm 0.05(f_0/t_0)$, the density of pinning centers (black open circles) $n_p = 1$, $f_{pv} = 10$, and $B = 0.2 B_{c2}$. The arrows indicate the evolution of the driving force. The inset is the velocity-force curve for the case of pure repulsion ($q = 0$), suggesting that the hysteresis arises due to intervortex attraction. (b) The vortex configuration (magenta solid circles) corresponding to labels A in the velocity-force curve shown in (a) at $F^L = 8 f_0$, and (c) the corresponding snapshot for label B (also at $F^L = 8 f_0$).

calculate the velocity-force curve for $q = 0$ (other parameters are the same as those for $q = 2.3$), as shown in the inset of Fig. 4(a). It can be seen that no hysteresis is observed for the pure repulsion system.[32] Thus, we conclude that this hysteretic behavior arises to be due to the dynamical reordering relating to intervortex attraction.

IV. CONCLUSIONS

In summary, based on a model system appropriate for vortex matter in low-κ type-II superconductors, we have studied the dynamic phases at zero temperature as functions of pinning strength and driving force. In addition to pinned state and plastic flow for lower driving forces, we find the vortices show two distinct dynamic phases: ordered moving bubbles and ordered moving stripes for larger driving forces. The simulation shows the vortices inside bubble and stripe domains are disordered, indicating that order within each bubble (or stripe) cannot be introduced by a driving force. Moreover, we find that the vortex system shows a marked hysteresis in its velocity-force characteristic, which results from a dynamical stripe reordering due to intervortex attraction.

*xxb@nju.edu.cn

[1]M. Seul and D. Andelman, Science **267**, 476 (1995).

[2]T. Garel and S. Doniach, Phys. Rev. B **26**, 325 (1982).

[3]C. Sagui and R. C. Desai, Phys. Rev. E **49**, 2225 (1994).

[4]L. Q. Chen and A. G. Khachaturyan, Phys. Rev. Lett. **70**, 1477 (1993).

[5]M. Seul and R. Wolfe, Phys. Rev. A **46**, 7519 (1992).

[6]B. P. Stojković, Z. G. Yu, A. R. Bishop, A. H. Castro Neto, and N. Grønbech-Jensen, Phys. Rev. Lett. **82**, 4679 (1999).

[7]R. P. Huebener, *Magnetic Flux Structures in Superconductors* (Springer-Verlag, New York, 1979).

[8]H. Träuble and U. Essmann, Phys. Status Solidi B **20**, 95 (1967).

[9]U. Essmann, Phys. Lett. A **41**, 477 (1972).

[10]E. H. Brandt, Rep. Prog. Phys. **58**, 1465 (1995).

[11]V. Moshchalkov, M. Menghini, T. Nishio, Q. H. Chen, A. V. Silhanek, V. H. Dao, L. F. Chibotaru, N. D. Zhigadlo, and J. Karpinski, Phys. Rev. Lett. **102**, 117001 (2009); E. H. Brandt and S. P. Zhou, Physics **2**, 22 (2009).

[12]V. O. Dolocan, C. Veauvy, F. Servant, P. Lejay, K. Hasselbach, Y. Liu, and D. Mailly, Phys. Rev. Lett. **95**, 097004 (2005).

[13]B. Obst, Phys. Status Solidi B **45**, 467 (1971).

[14]E. Babaev and M. Speight, Phys. Rev. B **72**, 180502(R) (2005).

[15]E. Babaev, J. Carlstrom, and M. Speight, Phys. Rev. Lett. **105**, 067003 (2010).

[16]A. E. Jacobs, Phys. Rev. B **4**, 3029 (1971).

[17]I. Luk'yanchuk, Phys. Rev. B **63**, 174504 (2001).

[18]F. Mohamed, M. Troyer, G. Blatter, and I. Luk'yanchuk, Phys. Rev. B **65**, 224504 (2002).

[19]X. B. Xu, H. Fangohr, S. Y. Ding, F. Zhou, X. N. Xu, Z. H. Wang, M. Gu, D. Q. Shi, and S. X. Dou, Phys. Rev. B **83**, 014501 (2011).

[20]See, e.g., X. B. Xu, H. Fangohr, X. N. Xu, M. Gu, Z. H. Wang, S. M. Ji, S. Y. Ding, D. Q. Shi, and S. X. Dou, Phys. Rev. Lett. **101**, 147002 (2008).

[21]See, e.g., A. B. Kolton, D. Domínguez, and N. Grønbech-Jensen, Phys. Rev. Lett. **83**, 3061 (1999).

[22]H. Fangohr, A. Price, S. Cox, P. A. J. de Groot, G. J. Daniell, and K. S. Thomas, J. Comput. Phys. **162**, 372 (2000).

[23]H. Fangohr, S. J. Cox, and P. A. J. de Groot, Phys. Rev. B **64**, 64505 (2001).

[24]H. J. Jensen, A. Brass, A. C. Shi, and A. J. Berlinsky, Phys. Rev. B **41**, 6394 (1990).

[25]C. Reichhardt, C. J. Olson, J. Groth, S. Field, and F. Nori, Phys. Rev. B **53**, R8898 (1996).

[26]K. Moon, R. T. Scalettar, and G. T. Zimanyi, Phys. Rev. Lett. **77**, 2778 (1996).

[27]F. Pardo, F. de la Cruz, P. L. Gammel, E. Bucher, and D. J. Bishop, Nature (London) **396**, 348 (1998).

[28]C. J. Olson, C. Reichhardt, and F. Nori, Phys. Rev. Lett. **81**, 3757 (1998).

[29]A. E. Koshelev and V. M. Vinokur, Phys. Rev. Lett. **73**, 3580 (1994).

[30]T. Giamarchi and P. Le Doussal, Phys. Rev. Lett. **76**, 3408 (1996).

[31]C. Reichhardt, C. J. O. Reichhardt, I. Martin, and A. R. Bishop, Phys. Rev. Lett. **90**, 026401 (2003).

[32]X. B. Xu, Y. Liu, H. Fangohr, L. Zhang, S. Y. Ding, Z. H. Wang, S. L. Liu, G. J. Wu, and H. M. Shao, Phys. Rev. B **73**, 214521 (2006).